OPTICAL AND NUMERICAL MODELING OF A SPATIAL HETERODYNE LASER-INDUCED BREAKDOWN SPECTROMETER

Dávid J. Palásti[1,2], Miklós Veres[3], Miklós Füle[4,5], Gábor Galbács[1,2]*

[1]Department of Inorganic and Analytical Chemistry, Faculty of Science and Informatics, University of Szeged, 6720 Dóm square 7, Szeged, Hungary
[2]Department of Materials Science, Interdisciplinary Excellence Centre, University of Szeged, Dugonics square 13, 6720 Szeged, Hungary
[3]Department of Applied and Nonlinear Optics, Institute for Solid State Physics and Optics, Wigner Research Centre for Physics, 1121 Konkoly-Thege Miklós way 29-33, Budapest, Hungary
[4]Institute of Physics, Faculty of Engineering, University of Szeged, 6724 Mars square 7, Szeged, Hungary
[5]ELI-HU Non-Profit Ltd., Wolfgang Sandner u. 3., H-6728 Szeged, Hungary
**e-mail: galbx@chem.u-szeged.hu*

1. INTRODUCTION

Spatial heterodyne spectroscopy (SHS) is one the several interferometric spectrometers proposed in the literature. It combines dispersion- and interference-based techniques. Basically it is a version of the Michelson interferometer with no moving parts and diffraction gratings in the place of mirrors. The radiation from a light source is collimated and split between two arms of the interferometer terminated by diffraction gratings. The light dispersed by the gratings recombines at the beamsplitter and produces Fizeau fringes that are recorded by an imaging detector. The wavelength-resolved information is thus converted to a spatially-resolved interferogram, from which the recovery of the spectrum is done by Fourier transformation.

The earliest practical realization of SHS with a useful spectral resolution was presented by Dohi and Suzuki [Dohi 1971], who applied a photographic plate as an imaging detector. Harlender was the first to describe the modern version of the SHS; he used a CCD camera as the detector and also developed algorithms for interferogram processing [Harlender 1991]. For a more detailed description of the SHS principle, please see e.g. [Harlender 1991, Lenzner 2016, Gojani 2019].

Only three full papers were published so far on the combination of SHS with laser-induced breakdown spectroscopy (LIBS). The shared compact and single-shot character make SHS and LIBS a perfect couple in theory. It was Gornushkin et al. who first proposed and tested the SHS-LIBS combination [Gornushkin 2014] as an instrumentation that has potential for sensitive, stand-off quantitative elemental analysis and sample classification applications. Angel et al. successfully demonstrated that the enhanced sensitivity of a miniature LIBS-SHS system is indeed adequate to perform stand-off analysis from a distance of 20 meters using no collection optics [Barnett 2017, Allen 2018].

In our present project, we are in the process of constructing a tunable, optimized SHS setup for LIBS use [Palásti 2019]. Now we present results from optical and numerical modeling which allow insight into the effect of the most important optical parameters of the setup on the spectroscopy performance.

2. EXPERIMENTAL

The optical model of the double grating SHS arrangement was constructed in Comsol Multiphysics, using the geometrical optics interface and the ray tracing module. A parametric sweep of non-sequential ray tracing was performed using hexapolarly arranged, unpolarized, monochromatic and collimated input light beam consisting of 331 individual rays, with plane wave approximation. Reflective grating parameters were used in the models (150, 300 and 600 mm^{-1} ruled gratings blazing at 500 nm). The plane of the grating surface was vertically aligned (there was no tilt) and the square-shaped detector was always placed at the same distance from the center of the beamsplitter as the gratings. The fundamental experimental variables of the SHS setup were the grating arm lengths (distance of the grating surface from the active plane of the beamsplitter; varied here as 50, 75 and 100 mm), grating rotation angle (around an axis oriented along the *z* direction and placed at the grating surface, measured counterclockwise from the grating to beamsplitter optical axis; here varied between 65 to 90 degrees), input beam wavelength, and input beam diameter. The gratings were used in the first diffraction order and the beam diameter as well as the detector size was kept at 20 mm. A schematic of the Comsol optical model can be seen in **Figure 1**. Lens tubes were added to the setup in order to block stray rays.

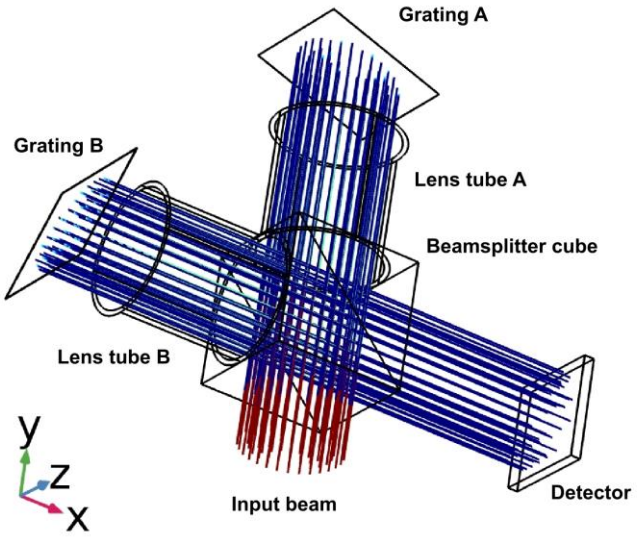

Figure 1. Conceptual ray tracing model of the SHS setup in Comsol.

3. RESULTS AND DISCUSSION

3.1. Spectral coverage and sensitivity

From an analytical point of view, the spectral coverage (SC), and more importantly the free spectral bandpass (FSB), of a spectrometer is crucial, because it directly limits the spectral information that can be collected. In our study, the FSB of the SHS arrangement was estimated by using ray tracing with a parameter sweep for the input beam wavelength (400 to 700 nm) and assessing the range of wavelength in which the first order output at the detector is free from contribution (overlap) from the second order diffraction. The gratings were fixed at their Littrow angle (Θ_L). We defined SC as the wavelength range between the 10% points of the relative sensitivity curve of the setup in the first order (between the maximum and minimum wavelengths for which the relative sensitivity is at least 10%).

It was found that the SC generally becomes consistently narrower with the increase of the grating density and the arm length. The FSB is 100-200 nm and is always significantly narrower than the spectral coverage, except for the 600 mm^{-1} grating, in which case FSB is equal to SC. The center position of FSB decidedly shifts towards shorter wavelengths with the increase of the two control parameters. The FSB is the widest (200 nm) for the 300 mm^{-1} grating, but is not much narrower for the 600 mm^{-1} grating with shorter arm lengths. In general, FSB seems to increase with the arm length for less dense gratings, whereas the trend is reversed for the 600 mm^{-1} grating. These findings indicate that it is generally mandatory to use optical filters in a compact SHS setup, primarily for order-sorting purposes, strategically placed at the input. Please also note that in order to exploit this FSB in LIBS spectroscopy, where a minimum of 100 pm spectral resolution is needed, the use of a megapixel detector is mandatory.

Apart from the transmission and reflectance characteristics of the optical elements used, the sensitivity of the SHS setup is expected to be influenced by the fraction of rays reaching the detector depending on the grating density, rotation angle and grating arm length. The relative sensitivity at the blazing wavelength is maximal at the Littrow angle, as expected. The relative sensitivity decreases rapidly, if the gratings are rotated concertedly; a few degree rotation results in a sensitivity drop of about 50%. Due to the same blazing wavelength, blaze angle (and hence Θ_L) changes linearly with the grating density. The trend is unaffected by the arm length. This indicates that according to the expectations, the highest sensitivity can be achieved if the gratings are fixed at Θ_L.

For geometric reasons, the sensitivity (fraction of rays reaching the detector) also depends on the relative size of the input beam and the detector, as well as the wavelength. This is well illustrated by **Figure 2**. In these ray tracing simulations, we kept the detector size fixed at 20 mm, and varied the other two parameters. As it can be seen, a decrease of the input beam diameter (assuming the same photon flux) increases the relative sensitivity and makes its wavelength-dependence less pronounced. The reason behind this is that a smaller diffracted beam can be better accommodated by the

detector than a large beam. At the same time, the decrease of the beam diameter also decreases the spectral coverage. In terms of wavelength, the maximum sensitivity is reached at around the 500 nm blaze wavelength), as expected. A similar trend was observed for other gratings and arm length values too.

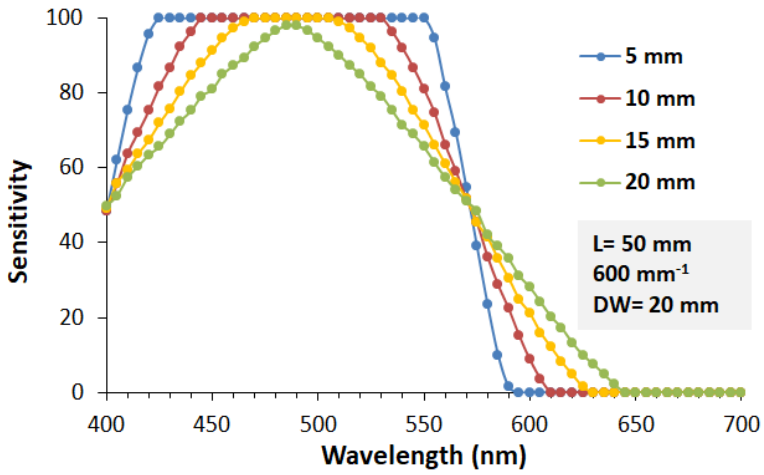

Figure 2. Effect of the wavelength and input beam diameter on the relative sensitivity of the SHS arrangement. The detector size is 20 mm.

A better comparison of the overall sensitivity of setups with different arm lengths and grating densities can be done via the calculation of the total intensity (cumulative fraction of rays) reaching the detector within the FSB. Our calculations clearly showed that the sensitivity is best for the 300 mm^{-1} grating, even if total intensities are normalized with the width of the FSB. It is a somewhat surprising finding, as considering that the blazing wavelength for the gratings used here is 500 nm, and the grating efficiency is known to be greatest around this wavelength, therefore the 600 mm^{-1} grating, for which the FSB is roughly centered around 500 nm, was expected to be optimal from the point of view of sensitivity.

3.2. Time dispersion

Under typical and single-pulse conditions, ns LIBS of a solid sample produces a plasma with a lifetime on the order of some tens of μs. If bulk liquid ns LIBS analysis is performed, the plasma lifetime is roughly an order of magnitude shorter. If a fs laser is used to generate the LIB plasma, then its lifetime is in the ns range. LIBS uses gated detection in order to minimize continuum background radiation, hence the required gating width is often one or two orders of magnitude shorter than the plasma lifetime. The above conditions require a detailed investigation of the time dispersion caused by the SHS arrangement as well as the means of coupling of the plasma light into the interferometer in order to determine the limiting condition and the best possible time resolution of the LIB-SHS system.

First, the time dispersion occurring inside the SHS itself needs to be considered. Dispersion will mainly occur because rays, depending on their relative position within the beam, will reach the detector at different times due the rotation of the gratings. In addition, different wavelengths will also travel through paths of slightly different length. Ray tracing simulation for all our modeled SHS arrangements indicate that the dispersion within the SHS arrangement is always quite small in our system: it varies between 2.4 and 27.9 ps. As expected, the dispersion scales linearly with the beam diameter, but the effect of wavelength and grating parameters is complex.

The evaluation of the effect of the means of light coupling into the SHS requires detailed analysis. The application of fiber optic light coupling is expected to deteriorate the time resolution of the LIB-SHS system, because chromatic, modal and waveguide dispersion in an optical fiber result in a distortion of the transmitted fast optical pulses. Our calculations revealed that the total dispersion under the experimental conditions used here (gratings, arm length, typical LIBS fiber optic cables, etc.) is between 150 and 342 ps. Clearly, the total dispersion in the optical fiber can be minimized by keeping the fiber length and the NA as small as possible.

It should also be mentioned that dispersion also occurs during the coupling of the plasma emission into the optical fiber and also at the collimation of the light output from the fiber. For the sake of simplicity, let us assume a two-lens light collection arrangement at the fiber input and a single collimation at the output, with identical lenses NA-matched to the fiber. Then the dispersion due to the different path lengths the light travels through the lenses will be proportional to the beam diameter. In total, the calculation gives increasing dispersion values for increasing beam diameters, but these values are only a couple of percents of the total dispersion occurring in the optical fiber.

Overall, it can be stated that the dispersion of pulsed light in the SHS arrangement alone is very small compared to the dispersion that occurs in the optical fiber, if the LIB plasma emission is coupled into the SHS arrangement via a fiber. In this case, the shortest gate width that can be used at the imaging detector is about 0.2-0.4 ns.

4. CONCLUSIONS

We have provided detailed numerical and optical modeling data on the sensitivity, free spectral range and time dispersion characteristics of a dual-grating SHS spectrometer meant for its optimization for LIBS use. It was shown that for high time resolution (e.g. ps) spectroscopy, direct coupling of the light into the spectrometer is advised, but for ns LIBS, fiber optic coupling is completely feasible. The free spectral range was found to be decent (100-200 nm) of the SHS even in a compact size, but to exploit this range for LIBS spectroscopy, where a minimum of 100 pm spectral resolution is needed, the use of a megapixel detector is mandatory.

5. ACKNOWLEDGEMENTS

The financial support received from various sources including the Ministry of Innovation and Technology (through project No. TUDFO/47138-1/2019-ITM FIKP) and the National Research, Development and Innovation Office (through projects No. K_129063, EFOP-3.6.2-16-2017-00005, TKP 2020 Thematic Excellence Program 2020) of Hungary are kindly acknowledged. The project was also supported by the ÚNKP-20-3 – New National Excellence Program of The Ministry for Innovation and Technology from the source of The National Research, Development and Innovation Fund.

6. REFERENCES

[Dohi 1971] T. Dohi, T. Suzuki, *Appl. Opt.*, 10 (1971) 1137.

[Harlender 1991] J. M. Harlander, Spatial heterodyne spectroscopy: interferometric performance at any wavelength without scanning, PhD dissertation, University of Wisconsin (USA), 1991.

[Lenzner 2016] M. Lenzner, J. C. Diels, *Opt. Express*, 24 (2016) 1829.

[Gojani 2019] A. B. Gojani, D. J. Palásti, A. Paul, G. Galbács, I. B. Gornushkin, *Appl. Spectrosc.*, 73 (2019) 1409.

[Gornushkin 2014] I. B. Gornushkin, B. W. Smith, U. Panne, N. Omenetto, *Appl. Spectrosc.*, 68 (2014) 1076.

[Barnett 2017] P. D. Barnett, N. Lamsal, S. M. Angel, *Appl. Spectrosc.*, 71 (2017) 583.

[Allen 2018] A. Allen, S.M. Angel, *Spectrochim. Acta B*, 149 (2018) 91.

[Palásti 2019] D. J. Palásti, L. Himics, T. Váczi, M. Veres, I. B. Gornushkin, G. Galbács, poster presentation #PI_010, *10th Euro-Mediterranean Symposium on LIBS*, Brno, 2019.